

NUMERICAL SIMULATION OF PATTERN FORMATION IN GRAIN FLOWS†

PIERRE-ALAIN GREMAUD*

Abstract. We present numerical computations for the flow of granular materials in hoppers. The algorithm is based on a cellular automaton approach and takes into account various microscopic effects, including “orientational effects”. The formation and the dynamics of density waves, recently discovered in physical experiments, is observed and analyzed computationally.

Key words. granular flow, automaton, discrete mechanics

AMS(MOS) subject classifications (1985 revision). 82C20, 73E50, 68Q80

1. Introduction. We consider in this paper the numerical computation of flows of rod-like materials, such as grass seeds. Recent experiments related to granular flows [3] have brought to the fore several phenomena that are not fully understood. Stress chains and porosity waves are some examples. Porosity or density waves, in particular, are believed to be at the origin of the violent vibrations which occasionally occur during the discharges of industrial silos. Those waves are basically thin low-density regions propagating through the material. The purpose of this work is to demonstrate the feasibility of a cellular automata approach for the computation of density waves and other pattern formations in granular flows, and to begin the study of dynamical models and the comparison of their solutions with experimental data.

Granular flows present several challenging issues. The continuum limit is more problematic than in fluid mechanics. Indeed, the “molecules” are much larger and the nature of the interactions between them has to be taken into account in some way. If elongated, non spherical grains, like grass seeds, are considered, the geometry and the orientation of the particles play a fundamental role, since additional torques appear. If faceted, rough sands are considered, it has been shown in some striking experiments [3] that complex “interlocking” leads in some cases to porosity waves that do not appear with smoother materials.

Orientation being easier to mathematically characterized than “roughness”, we will focus in this paper on the flow of thin grains in a hopper. Experimentally, at least two different regimes can be observed

†This work was supported in part by the Army Research Office through grant DAAH04-95-1-0419. Computing activity was partially supported by the North Carolina Supercomputing Center.

*Center for Research in Scientific Computation and Department of Mathematics, North Carolina State University, Raleigh, NC 27695-8205.

a slow regime: the material is glassy; energy is lost through friction as grains slide across each other; this behavior is usually believed to be associated with plasticity [3,19];

a fast regime: the material is close to a gas of particles; energy is lost through inelastic collisions.

During the discharge of a hopper, those two types of flows as well as a whole family of cross-over regimes can be observed, often simultaneously, at different locations in the hopper. At the same time, some other regions might be totally stagnant. The free surface at the top can also present complicated configurations. Finally, experiments often show long-range alignment of the grains over distances that are many particles long.

Modelling can be achieved by two different and, in our view, complementary methods, a continuum approach [10, 11, 20, 21, 22, 23, 24] and a discrete approach [1, 2, 3, 13, 14, 16, 25].

It is very difficult, in a continuum theory context, to properly take into account the above microscopic properties. Finding satisfactory constitutive relations is problematic. On the other hand, meaningful molecular dynamics approaches require a very large number of particles. In the case of non spherical particles, additional degrees of freedom are required in order to describe the orientation of the grains. Integrating the equations of motion becomes then very costly.

A very promising approach has been proposed in [2] where a discrete approximation of the molecular dynamics itself is considered, leading to cellular automata models. In this paper, we start from the point of view considered in [2] and develop a new “doubly discrete” model. First, particles are considered, as opposed to a continuum, and secondly, those particles can only take positions on a finite set of locations described by a lattice; furthermore the state of each particle, i.e., its orientation, is also quantized. Our model does not satisfy all the properties usually attached to cellular automata [28] in the sense that it is not deterministic, and that the information travels at a finite speed.

In this paper, we present computational evidences of the presence of density waves during hopper discharges. We are not aware of other results of this type.

Section 2 is devoted to the description of our discrete models. The numerical results are presented and discussed in Section 3. Finally, concluding remarks are offered in Section 4.

2. Automata as models of granular flows. Automata are discrete dynamical systems which give simple models for many complex systems containing large numbers of identical components with local interactions. There has been recently a lot of work towards the classification of divers types of automata [28]. Generally, an automaton consists of a lattice of sites. To each site corresponds a state which takes its values in some finite set,

typically integer numbers, or symbols. The states evolve in discrete time steps. At each site, the value is determined by the values at the neighboring sites, according to a set of local rules.

Automata seem to have been originally introduced in the 40's by, among others, J. von Neumann [26] in relation to biological self-reproduction. They have since then been used in order to model many complex systems from fluid dynamics [6, 8, 9, 29], to multiple applications in biology [12] or image processing (see [27] and [28] where many applications are discussed).

The main assumption in this paper is that granular flows, and their often extremely complicated structures, can be, at least qualitatively, modelled by cellular automata. Only two dimensional flows are considered.

Our automaton will be defined by

- the choice of a lattice (topology),
- the choice of state variables,
- the choice of a mode of updating (either synchronous, i.e. Jacobi-like, or Gauss-Seidel),
- the choice of local rules.

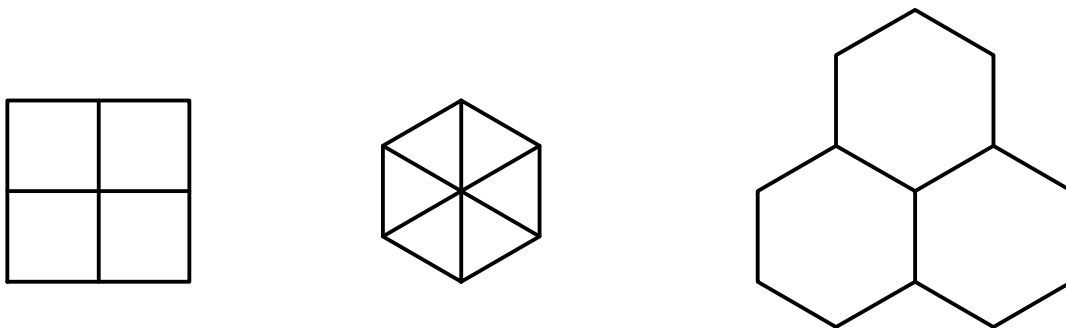


FIGURE 1. *Cells corresponding to the nearest neighbors for square (left), triangular (center) and hexagonal (right) lattices.*

a. Lattice. The two dimensional lattice is required to have rotational and translational symmetry about each site, or node. The possible configurations are then triangular (six nearest neighbors), square (four nearest neighbors) or hexagonal (three nearest neighbors), see Figure 1.

We use here a triangular lattice¹; the hexagonal cells defined by the nearest neighbors will play in our model a fundamental role. This choice is motivated by the two following reasons. First, as is well known, in case the particles are spherical the densest possible configuration in two dimensions is obtained on the triangular lattice [7, p.8], see Figure 2. This situation should be describable in the model.

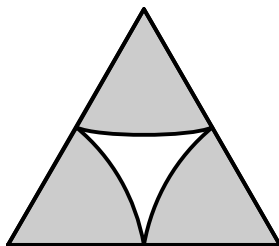


FIGURE 2. *Densest sphere packing, density = $\frac{\pi}{\sqrt{12}}$.*

Second, the large scale behavior of cellular automata can be approximated by suitable average rules for collections of particles. The rules of the automata can then be considered as finite difference approximations to partial differential equations describing the phenomenon under consideration at the macroscopic level. It can be shown that some simple two-dimensional cellular automata defined on the triangular lattice with hexagonal symmetry follow exactly the standard Navier-Stokes equations [8, 9, 17]. This however is not true if the square lattice is considered, since then spurious conservation laws appear as a result of a lack of isotropy of the lattice; Galilean invariance is not satisfied by the emerging equation.

For a given hopper and a given density of particles, we only consider the nodes of the lattice that belong to the closed domain defined by the shape and geometry of the hopper. The boundary conditions are implemented via suitable local rules.

b. State variables. The state variables correspond to the orientation of the particles. More precisely, at each node, the state has value 0, 1, 2, 3 or 4. The values 1, 2, 3 correspond to the orientation of the particle, the three values being related to the three “directions” of the lattice, see Figure 3. The values 0 and 4 indicate respectively that the corresponding site is empty or outside the hopper.

¹The triangular lattice is often referred to, in the literature, as the *hexagonal lattice*, because of its hexagonal symmetry!

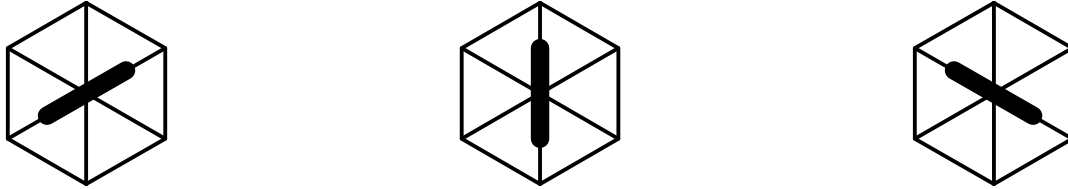


FIGURE 3. Orientation corresponding the state values 1, 2 and 3 (left, center and right).

c. Mode of updating. The mode of updating is Gauss-Seidel-like. For each time-step, a horizontal sweep, level by level, is considered. In order to avoid symmetry-breaking effects, the ordering according to which the particles in a given level are considered is randomly generated. A new ordering is constructed at each level. The new state at each node is determined according to a local energy minimization criterion defined by the local rules described below. Once the new state of a particle is determined, the global state vector, configuration, of the system is immediately updated.

d. Local rules. At each time step, all the sites are probed according to the ordering defined above, for “holes”, i.e. empty sites. Once an empty site is located, the state of the cell formed by its neighboring nodes is examined.

Let \mathbf{ILOC} be a 7-vector, where $\mathbf{ILOC}(i)$, $i=1, \dots, 7$, corresponds to the state of the node i according to the local numbering defined in Figure 4.

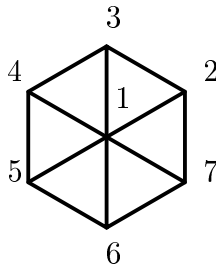


FIGURE 4. Local numbering.

If $\mathbf{ILOC}(2) = \mathbf{ILOC}(3) = \mathbf{ILOC}(4) = 0$, i.e. “holes in positions 2, 3 and 4”, nothing can fall into the hole in position 1 and the next site is considered. If however one of the sites 2, 3 or 4, above 1 which is empty, is occupied, then one of those particles will move to position 1. Each of the possible configuration is examined. To each configuration of the hexagonal cell is associated an energy. The new configuration is the one which has minimal energy, with random choice in case of a near tie.

The energy is designed to take into account effects related to local density variations, to the influence of the orientation of a grain on its direction of motion, to “inertia” and to interactions with the walls of the hopper, where needed. For each cell, we have then

$$E = E_D + E_O + E_I + E_W.$$

The relative strength of the four above effects is determined by corresponding positive parameters C_D , C_O , C_I , C_W . There is no gravitational part per se in the energy, since gravitational effects are already taken into account in the very construction of the model: the holes are filled, when possible.

Let us consider an empty node and the corresponding local vector `ILOC`. The candidate(s) for the new configuration of the hexagonal cell is denoted by `INEW`.

The density related part of the energy E_D comes from the fact that a moving grain will tend to favor the orientation already adopted by most of its new neighbors

```

ED = 0
FOR I=2,7
    IF (INEW(I) ≠ INEW(1) AND INEW(I) ≠ 4) ED = ED + CD
ENDFOR

```

If elongated particles are considered, they will have a tendency to move, or slide across each other in the “direction” of the particle itself. Motions along other directions are less likely to occur and would therefore correspond to higher energy configurations. If the falling particle has number i , in the local numbering

$$\text{ILOC} = [0 \quad \cdot \quad \star \uparrow_i \quad \cdot \quad \cdot \quad \cdot] \longrightarrow \text{INEW} = [\star \quad \cdot \quad 0 \uparrow_i \quad \cdot \quad \cdot \quad \cdot]$$

then we set

$$E_O = C_O | (I-1) - \text{ILOC}(I) |.$$



FIGURE 5. *Particles whose move to the center “costs” C_O (left) and $2C_O$ (right).*

The “inertial” effect takes into account the fact that energy is needed to rotate a particle

$$E_I = C_I | ILOC(I) - INEW(I) |,$$

where i is as above.

Finally, a particle next to a wall will tend to adopt an orientation as close as possible to that of the wall. If the state value 4 corresponds to “being outside the hopper”, we have then

$$\begin{aligned} \text{IF (INEW(5) = 4 AND INEW(1) } \neq \text{ 3) } E_W &= C_W \\ \text{IF (INEW(7) = 4 AND INEW(1) } \neq \text{ 1) } E_W &= C_W. \end{aligned}$$

Unless the hopper is one particle wide or less at some point, both cases cannot happen at once.

A hasty analysis of the above model might lead to the impression that, due to the systematic filling of the holes, the top free boundary developing during the discharge cannot present slopes larger than the slope trivially allowed by the lattice between two “nonvertical” neighbors, i.e. a 30° angle from the horizontal direction. This turns out to be incorrect; as shown in the example described in Figure 6, steep slopes can develop.

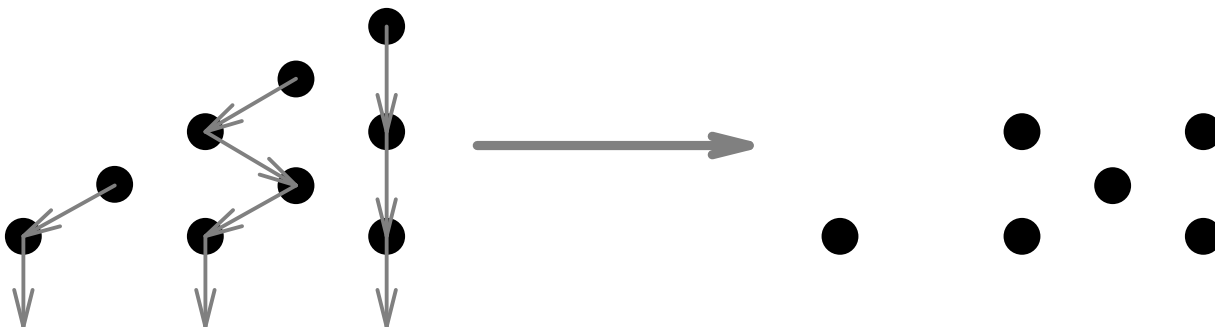


FIGURE 6. *Creation of a steep slope by elementary motion of the particles. The motions on the left, take place starting at the bottom.*

3. Numerical results. In this section, several numerical experiments based on the automaton model described above are discussed. Qualitative and quantitative comparisons with physical experiments are offered.

The parameters defining the hopper itself are

SLOPE: slope of the walls of the hopper,

N: number of sites at the lower opening (outlet),

L : number of levels of particles initially in the hopper.

The parameters defining the properties of the grains are the parameters C_D , C_O , C_I , C_W defined in section 2.

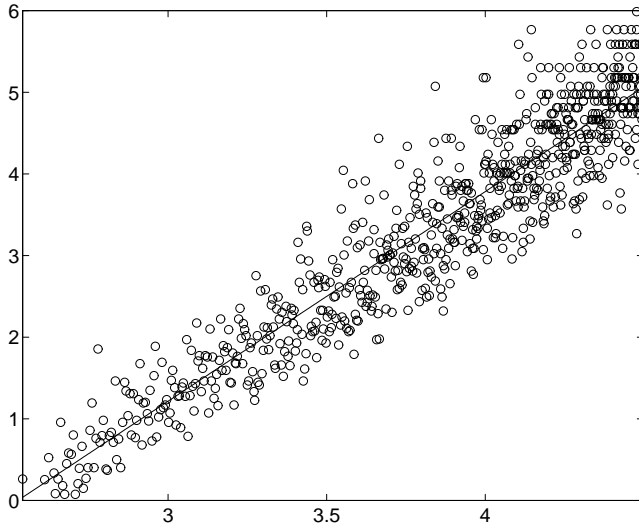


FIGURE 7. $\log \frac{1}{P}$ against $\log \theta$.

a. Stagnant regions. Experimental facts [3], as well as our computations indicate that unless the opening of the hopper is small (about 13° in our computations), two main domains are observable in the flow. The motion takes place near the center of the hopper, while the areas near the walls tend to be stagnant. Flows with a stagnant area are usually referred to as funnel flows, as opposed to flows without stagnant areas and so-called mass flows. The latter are preferred in applications [2].

The position of the interface between stagnant and moving regions gives us a simple quantitative way to check our model against both theoretical and experimental results. It has been predicted that for small enough hopper angles, there should always be mass flow [3], [19], or more precisely, the stagnant part of the flow would be outside the hopper.

In our numerical experiments, we measure, *along the side wall*, the position of the highest particle that has moved after a given number of iterations. This allows us to define a dimensionless parameter P corresponding to the proportion of the flow that is moving, i.e., non stagnant, measured along one side wall. In the results below, P is given as the average of the two values corresponding to each of the two side walls.

Let θ be the full opening of the hopper. Based on experiments [3] and theoretical studies [19] (see also the references quoted in [3]), we expect P to be near 1 (mass flow) for all angles less than a critical value θ_c , and P is expected to obey a power law for $\theta > \theta_c$. We have computed P every $\frac{1}{10}$ th degree for angles θ varying between 10° and 90° and

$C_D = 0.01$, $C_O = 0$, $C_I = 0.1$, $C_S = 0$, $C_W = 0.1$, $N = 20$, $L = 800$. In each case, P is measured after 100 iterations. An exponential fit

$$\frac{1}{P} = b\theta^a$$

of the data yields for a the value $a \approx 2.56$ which is in good agreement with the experimental value of $a = 2.2 \pm 0.1$ reported in [3]. A comparison of the values of the parameter b is not meaningful here because it is essentially a scaling factor. In Figure 7, we have reported $\log \frac{1}{P}$ vs $\log \theta$.

b. Flow rate. The rate of the flow of the particles from the hopper is another quantity allowing a quantitative evaluation of our model. It has been known for quite some time that the flow rate is *independent* of the quantity of material remaining in the hopper, unless this one is nearly empty (see e.g. [18] and the references therein about early experiments related to sand clocks). This behavior is in strong contrast with the case of a fluid, where a simple application of the Bernoulli's principle leads to a rate of flow proportional to the square root of the height of the fluid.

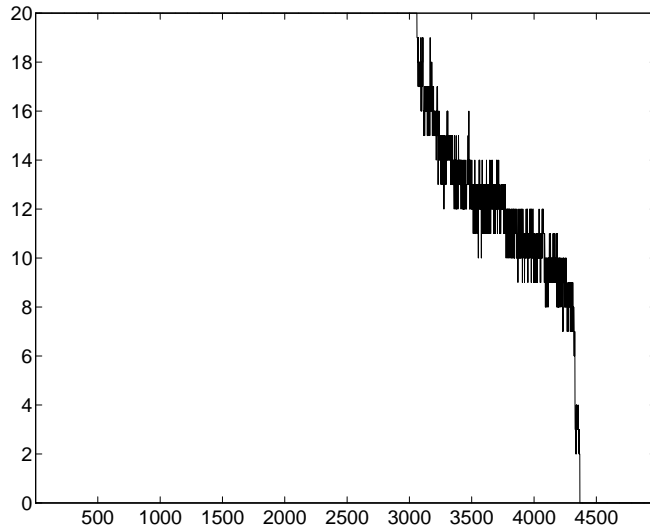


FIGURE 8. *Flow rate vs. number of iterations.*

c. Pattern formation. One of the main results in the experiments conducted by Behringer et al. [3] is that the structure of the flow depends strongly on the nature of the grains. It was observed that smooth sands, i.e. sands where effects related to orientation and/or roughness are thought to be negligible, exhibit only structureless flows.

We use an indirect characterization of the density, derived from the local rules. If a cell, or a more general domain, contains particles which (almost) all have the same orientation, the corresponding area is interpreted as dense. In the following figures, the colorcode corresponds to the three possible orientations of the particles.

Experiment 1. We first look at the role of the density related parameter C_D . In this experiment, all the other parameters are fixed, and have the following values: $n=20$, $L=800$, $\text{slope} = 3$, $C_O = 0$, $C_I = 0.1$, $C_W = 10$.

We display the results obtained after 500 iterations. In Figure 9, the three main types of behavior of the flow are presented. If the orientation effects are turned off, $C_D = C_O = 0$, the flux is structureless, see Figure 9.a. If the value of the density related coefficient C_D is increased, then various patterns appear. For $C_D = 0.01$, see Figure 9.b, horizontal structures appear. Each of those bands is composed almost exclusively of particles having the same orientation. For this opening of the hopper ($\text{slope} = 3$, and thus angle $\approx 36.9^\circ$), the bands are moving downwards with respect to the time, i.e. from one iteration to the next. If $C_D = 1$, the behavior is totally different, see Figure 9.c. The grains organized themselves in large patches of particles with identical orientation. The general structure is strongly reminiscent of the density waves observed by Behringer et al., see [3, Fig. 3.12, p.100], where large high-density zones are separated by thin areas or curves of small densities. *We postulate that those density waves correspond to the curves of separation between patches that can be observed in Figure 9.c.* For those values of the parameters, the “waves” are moving upward.

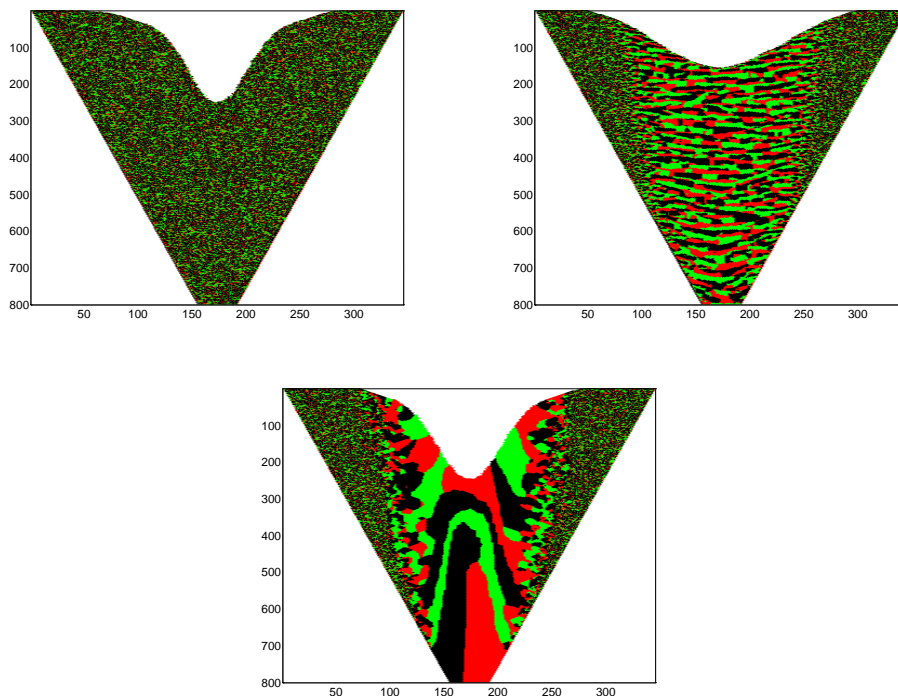


FIGURE 9. *Pattern formation for different values of C_D ; a: $C_D = 0$, b: $C_D = 0.01$, c: $C_D = 1$.*

The configuration observed in Figure 9.b, i.e. $C_D = 0.01$, is also the one obtained for any smaller positive value of this coefficient. In other words, the density related term kicks in as soon as C_D is not zero. The transition between the behaviors observed in Figure 9.b and 9.c is more involved. For $C_D = 0.01$, see Figure 9.b, the three possible orientations seem to be evenly distributed throughout the hopper, in both the stagnant and moving domains. However, if C_D is increased from 0.01 to 0.09, almost no particles with a vertical orientation are present in the moving zone, see Figure 10.a ($C_D = 0.09$). The respective patches are still moving downward. If slightly larger values of C_D are considered, $C_D = 0.095$, 0.098, 0.1, see Figure 10.b, 10.c, 10.d, respectively, then sets of particles oriented vertically are again observable. Remarkably, while the domains corresponding to the two non vertically oriented particles are still moving downward, the vertically oriented patches appear to be moving upward². If C_D is increased beyond 0.1, the horizontal band structure totally disappears; larger uniformly oriented upward moving domains are observable.

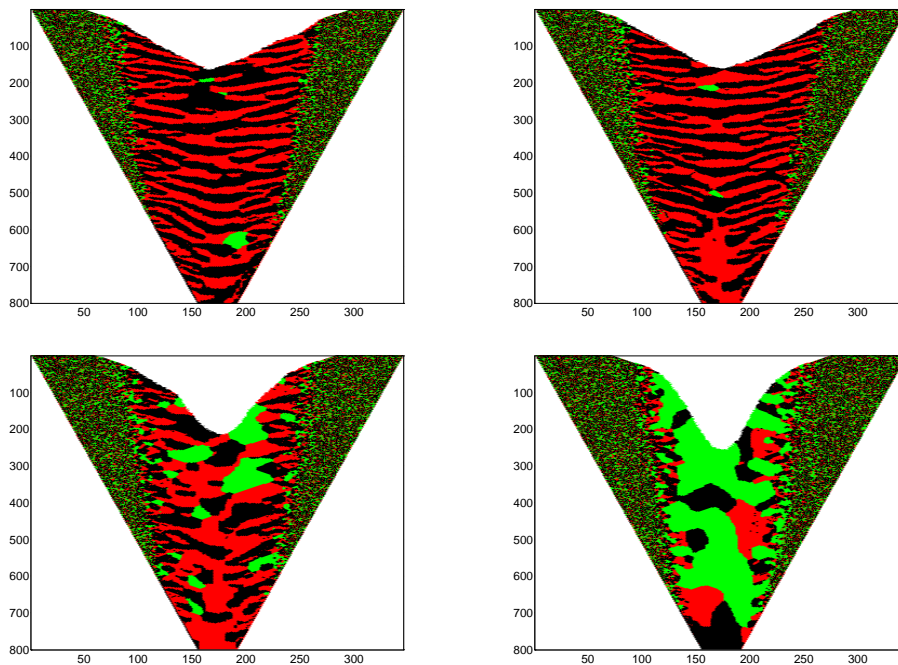


FIGURE 10. *Sensitivity of the formation of pattern with respect to C_D ; a: $C_D = 0.09$, b: $C_D = 0.095$, c: $C_D = 0.098$, d: $C_D = 0.1$.*

²The “orientation domains” only are moving upward, not the particles themselves, since such moves are by construction impossible in our simple model.

As seen in Figure 10.a, 10.b, 10.c, 10.d, the shape of the free boundary is also strongly dependent on C_D , at least within the range of values. We have at this point no explanation of the above phenomena.

Experiment 2. The algorithm being not fully deterministic, we have to expect some changes in the results if the pseudorandom number sequence used is changed. Starting from the *same* randomly generated initial condition, only small differences in the flow should appear between two runs of the algorithm, with two different pseudorandom sequences. We use here a generator of the type GFSR (generalized feedback shift register) with period $2^{251} - 1$, see [15, appendix]. Only the seed of the generator was changed from one run to the next.

The results are illustrated in Figures 11.a and 11.b and were obtained, after 500 iterations, with $n = 20$, $L = 800$, $\text{sLOPE} = 3$, $C_D = 1$, $C_O = 0$, $C_I = 0.1$, $C_W = 10$. The global nature of the two computed flows is the same. Indeed, the moving and stagnant regions are similarly located, the shape of the free surface is almost identical and in both cases, the pattern in the moving region is of similar, although clearly not identical, nature.

We now consider what happens if the same algorithm (same pseudorandom sequence) is used on slightly different initial conditions. We already know that the global nature of the flow is somewhat “robust”, i.e., it is not sensitive to small perturbations of the algorithm. Not surprisingly, as illustrated below, the same is true if small perturbations of the initial condition are considered instead.

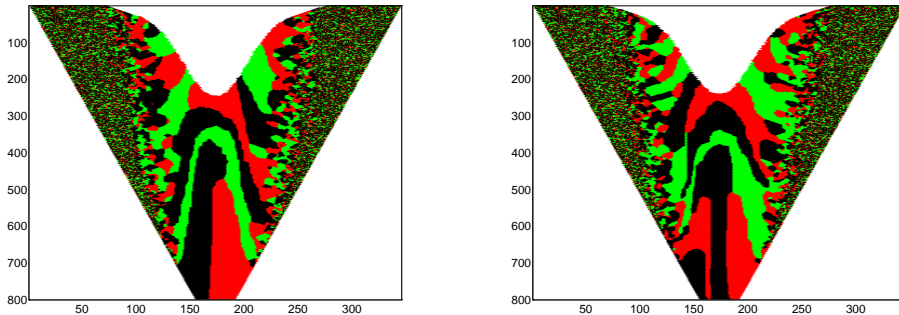


FIGURE 11. *Sensitivity with respect to the pseudorandom sequences used.*

The local structure of the flow, on the other hand, has been found to be sensitive to perturbations of the algorithm, see Figure 11. In Figures 12.a and 12.b, we have reported results obtained using the same pseudorandom sequence, with very small differences in the initial condition. The results are displayed after 100 iterations, and the values of the

parameters are $\mathbf{n} = 20$, $\mathbf{L} = 800$, $\mathbf{SLOPE} = 3$, $C_D = 0.5$, $C_O = 0$, $C_I = 0.1$, $C_W = 10$. In Figure 12.b, the initial condition disagrees with that of Figure 12.a at only four, randomly chosen, nodes, out of about 100,000. Those initial differences have resulted in serious changes in the local structure of the flow. If three or less nodes are changed, we did not observe any significant change in the flow, even over long periods.

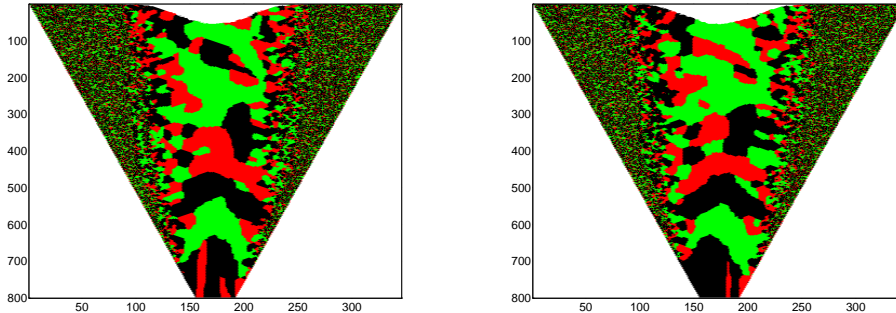


FIGURE 12. *Sensitivity with respect to the initial condition.*

The systems under study seem thus to be very sensitive, unstable in some sense, with respect to small perturbations of the initial condition.

Experiment 3. We look here at the role of the parameter C_O related to the relationship between the orientation of a grain and its direction of motion. The presence of the term E_O in the energy functional E puts much more emphasis on the orientation of the particles. The configuration of the flow is found to be extremely sensitive to changes of the parameter C_O .

In the following results in Figure 13, shown after 500 iterations, the following parameters are fixed $\mathbf{n} = 20$, $\mathbf{L} = 800$, $\mathbf{SLOPE} = 3$, $C_D = 0.5$, $C_I = 0.1$, $C_W = 10$. Figures 13.a and 13.b correspond to $C_O = 0.0009$ and $C_O = 0.0010$

We observe that the shape of the free surface is now much more complicated. Even though, complicated free surfaces are observed experimentally in many cases, giving a full justification of the above results is not clear. If we consider larger values of C_O , clearly non physical and highly asymmetrical configurations are obtained. The initial nonuniformities seem to be enlarged by the algorithm, and the system driven away from even remotely symmetric configurations. If C_O is smaller ($C_O \lesssim 0.0005$), the term E_O has almost no influence in the minimization process.

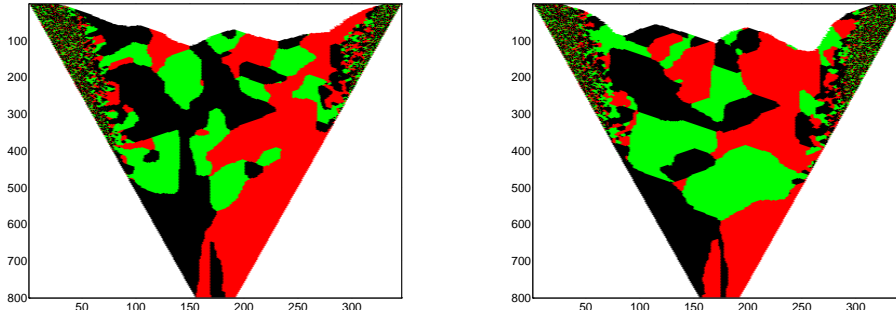


FIGURE 13. *Configuration of the flow for a: $C_O = 0.0009$, b: $C_O = 0.0010$.*

4. Conclusions. We have proposed and tested a cellular automaton, modelling the flow of granular material in a hopper. The approach is extremely simple and has been shown to allow, at least partially, the computational study of elusive phenomena which have largely escaped numerical approximation. More precisely, the numerical results reported here present many common features with experimental results such as presence/absence of stagnant regions as a function of the shape (opening) of the hopper, shape of the free surface consistent, in many cases, with what can be observed in experiments, development and propagation of low density waves through the material.

The main limitation of this approach is that it is, at least at this point, purely qualitative. Among all the possible values of the several parameters at hand in the model, only a small subset corresponds to physical situations. Without more information about a quantitative, physical, interpretation of the numerical results, finding the “reasonable values” is not evident. However, to some extent, the above shortcomings are shared by molecular dynamics approaches and by continuum approaches (lack of satisfactory constitutive relations). A more realistic model should also probably treat differently the particles which are part of the free surface and those which are in the middle of the flow.

Suitable averaging rules should lead to quantitative links between variables in discrete mechanics models and macroscopic quantities. Results of the type have been obtained in [4] where hydrodynamic limits of particle systems are considered, leading to nonlinear singular diffusion equations for the local density (see also [5]). Those studies are however purely one-dimensional.

Finally, although our simulations are two dimensional, we believe that they capture many of the essential mechanisms observed in three-dimensional experiments.

Acknowledgments. It is a pleasure to thank here Bob Behringer from Duke University for several helpful and enlightening conversations, and Bruce Loftis, from the North Carolina Supercomputing Center for the interest he has taken in this work.

REFERENCES

- [1] BARKER, G.C. (1994). Computer simulations of granular materials. In Metha, A. (ed.), *Granular matter: an interdisciplinary approach*, Springer-Verlag, pp. 35–83.
- [2] BAXTER, G.W., AND BEHRINGER, R.P. (1991). Cellular automata models for the flow of granular materials. *Physica D* **51**, 465–471.
- [3] BEHRINGER, R.P., AND BAXTER, G.W. (1994). Pattern formation and complexity in granular flows. In Metha, A. (ed.), *Granular matter: an interdisciplinary approach*, Springer-Verlag, pp. 85–119.
- [4] CARLSON, J.M., GRANNAN, E.R., SWINDLE, G.H., AND TOUR, J. (1993). Singular diffusion limits of a class of reversible self-organizing particle systems. *An. Prob.* **121**, 1372–1393.
- [5] CHAYES, J.T., OSHER, S.J., AND RALSTON, J.V. (1993). On singular diffusion equations with applications to self-organized criticality. *Comm. Pure Appl. Math.* **46**, 1363–1377.
- [6] CHEN, S., WANG, Z., SHAN, X., AND DOOLEN, G.D. (1992). Lattice Boltzmann computational fluid dynamics in three dimensions. *J. Stat. Phys* **68**, 379–400.
- [7] CONWAY, J.H., AND SLOANE, N.J.A. (1993). *Sphere packings, lattices and groups*, 2nd ed, Springer-Verlag.
- [8] FRISCH, U., D’HUMIÈRES, D., HASSLACHER, B., LALLEMAND, P., POMEAU, Y., AND RIVET, J.-P. (1987). Lattice gas hydrodynamics in two and three dimensions. *Complex Systems* **1**, 649–707. See also Doolen, G.D. (ed.) (1990), *Lattice gas methods for partial differential equations*, Addison-Wesley, 77–135.
- [9] FRISCH, U., HASSLACHER, B., AND POMEAU, Y. (1986). Lattice-gas automata for the Navier-Stokes equation. *Phys. Rev. Lett.* **56**, 1505–1508.
- [10] GARAIZAR, F.X., AND SCHAEFFER, D.G. (1992). Numerical computations for shear bands in an antiplane shear model. *Preprint CRSC-TR92-19*, North Carolina State University.
- [11] GARDNER, C.L., AND SCHAEFFER, D.G. (1994). Numerical simulation of uniaxial compression of a granular material with wall friction. *SIAM J. Math. Appl.* **54**, 1676–1692.
- [12] GREEN, D.G. (1993). Emergent behaviour in biological systems. In Green, D.G., and Bossomaier, T. (eds.), *Complex systems: from biology to computation*, IOS Press, pp. 24–35.
- [13] HAFF, P.K. (1994). Discrete Mechanics. In Mehta, A. (ed.), *Granular matter: an interdisciplinary approach*, Springer-Verlag, pp. 141–160.
- [14] MEHTA, A. (1994). *Granular matter: an interdisciplinary approach* Springer-Verlag.
- [15] RIPLEY, B.D. (1990). Thoughts on pseudorandom number generators. *J. Comput. Appl. Math.* **31**, 153–163.
- [16] RISTOW, G.H., AND HERRMANN, H.J. (1994). Density patterns in two-dimensional hoppers. *Physical Review E* **50**, pp. R5–R8.
- [17] SALEM, J.B., AND WOLFRAM, S. (1986). Thermodynamics and hydrodynamics with cellular automata. In Wolfram, S. (ed.), *Theory and applications of cellular automata*, World Scientific, pp. 362–365.
- [18] SAVAGE, S.B. (1993). Disorder, diffusion and structure formation in granular flows. In Bideau, D., and Hansen, A. (eds.), *Disorder and granular Media*, North-Holland, pp. 255–285.
- [19] SCHAEFFER, D.G. (1987). Instability in the evolution equations describing incompressible granular flow. *J. Diff. Eq.* **66**, 19–50.
- [20] SCHAEFFER, D.G. (1990). Mathematical issues in the continuum formulation of slow granular flow. In Joseph, D.G., and Schaeffer, D.G. (eds.), *Two phase flows and waves*, Springer-Verlag, pp. 118–129.
- [21] SCHAEFFER, D.G., AND SHEARER, M. (1993). Unloading near a shear band: a free boundary problem for the wave equation. *Comm. Part. Diff. Eq.* **18**, 1271–1298.

- [22] SHEARER, M., GARAIZAR, F.X., SCHAEFFER, D.G., AND TRANGENSTEIN, J. (1993). Formation and development of shear bands in granular material. *Preprint CRSC-TR93-16*, North Carolina State University.
- [23] SHEARER, M., AND SCHAEFFER, D.G. (1993). The initial value problem for a system modelling unidirectional longitudinal elastic-plastic waves. *SIAM J. Math. Anal.* **24**, 1111-1144.
- [24] SHEARER, M., AND SCHAEFFER, D.G. Unloading near a shear band in granular material. *Quart. Appl. Math.*, to appear.
- [25] THOMPSON, P.A. Granular materials in tall silo: a reexamination of Janssen's theory from a molecular-dynamics perspective. In preparation..
- [26] VON NEUMANN, J. (1963). The general and logical theory of automata. In Taub, A.H. (ed.), *John von Neumann, Collected Works, Volume V*, Pergamon Press. pp. 288-328.
- [27] WEISBUCH, G. (1991). *Complex systems dynamics*, Addison-Wesley.
- [28] WOLFRAM, S. (1986). *Theory and applications of cellular automata*, World Scientific.
- [29] WOLFRAM, S. (1990). Cellular automaton fluids 1: basic theory. *J. Stat. Phys.* **45**, 471-526. See also Doolen, G.D. (ed.) (1990), *Lattice gas methods for partial differential equations*, Addison-Wesley, pp. 19-73.